

Requirement for *Atm* in Ionizing Radiation-Induced Cell Death in the Developing Central Nervous System

Karl-Heinz Herzog, Miriam J. Chong, Manuela Kapsetaki, James I. Morgan, Peter J. McKinnon*

Ataxia telangiectasia (AT) is characterized by progressive neurodegeneration that results from mutation of the *ATM* gene. However, neither the normal function of ATM in the nervous system nor the biological basis of the degeneration in AT is known. Resistance to apoptosis in the developing central nervous system (CNS) of *Atm*^{-/-} mice was observed after ionizing radiation. This lack of death occurred in diverse regions of the CNS, including the cerebellum, which is markedly affected in AT. In wild-type, but not *Atm*^{-/-} mice, up-regulation of p53 coincided with cell death, suggesting that *Atm*-dependent apoptosis in the CNS is mediated by p53. Further, p53 null mice showed a similar lack of radiation-induced cell death in the developing nervous system. *Atm* may function at a developmental survival checkpoint that serves to eliminate neurons with excessive DNA damage.

Ataxia telangiectasia is a hereditary multisystemic disease resulting from mutations of *ATM* (1) and is characterized by progressive neurodegeneration, cancer, immune system defects, and hypersensitivity to ion-

izing radiation (2–4). ATM is similar at its COOH-terminal region to the phosphoinositol 3-kinase family, suggesting a role in signal transduction (2). Moreover, *in vitro* studies have shown that ATM is a component of the cell cycle checkpoint machinery that causes growth arrest after ionizing radiation-induced DNA damage (2, 5). Although defects in ATM lead to neurodegeneration, its physiological role in the nervous system is unclear (6). The neurological defect or defects in AT become apparent early in life, suggesting that they originate

during development. Furthermore, *Atm* is highly expressed in the developing nervous system, but only at low levels in the adult CNS (7).

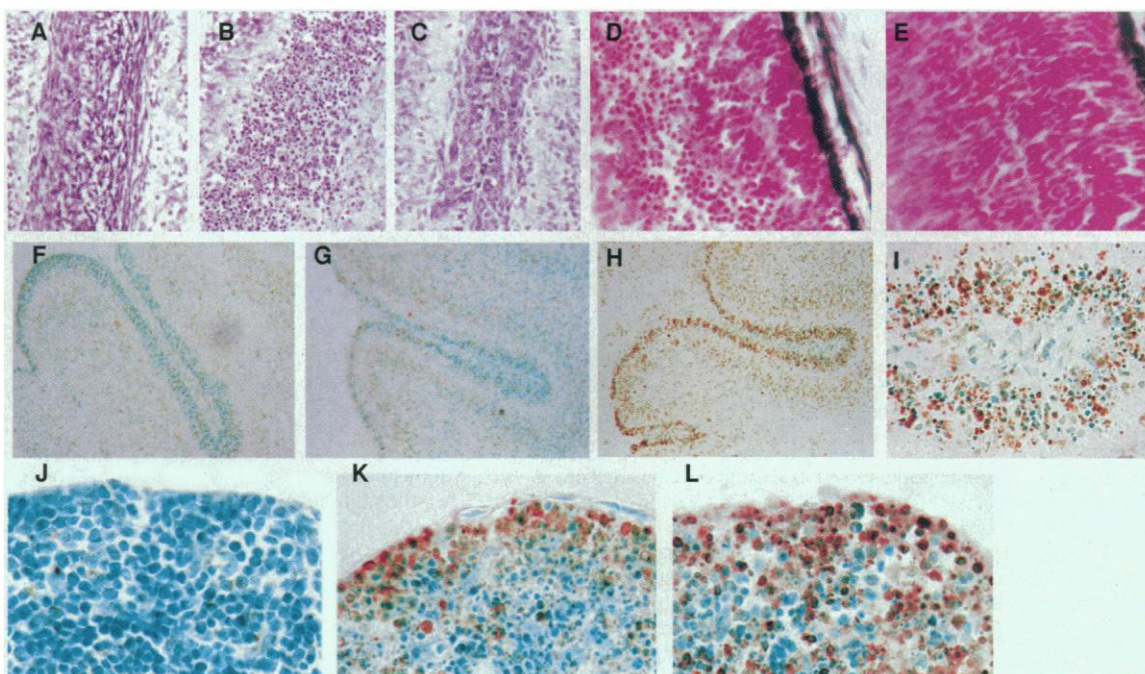
We generated an *Atm*-knockout mouse by deleting a region of *Atm* that included exons 57 and 58 (8). These *Atm*^{-/-} mice had a similar phenotype to that of other recently reported *Atm*^{-/-} mice, including sterility and proneness to lymphoma (9). In many regions of the CNS in *Atm*^{-/-} mice, ionizing radiation failed to induce cell death (10). There was an almost complete absence of irradiation-induced cell death in the hippocampal dentate gyrus, retina, cerebellum, and cerebral cortex compared with wild-type (WT) tissues (Fig. 1). In WT mice, irradiation of the external granule layer (EGL) of the cerebellum resulted in widespread cell death, whereas the EGL of *Atm*^{-/-} mice showed only occasional dead cells. In contrast, the thymus showed similar susceptibility to irradiation in both WT and *Atm*^{-/-} mice. As an independent measure of cell death, *in situ* end labeling (ISEL) was used (11). ISEL-positive cells were seen in the WT, but not *Atm*^{-/-} CNS after irradiation (Fig. 1). Apoptosis in the thymus occurred in both the WT (Fig. 1K) and *Atm*^{-/-} (Fig. 1L) mice, indicating that the cellular machinery responsible for apoptosis-associated DNA degradation is present in *Atm*^{-/-} mice.

To establish that the *Atm*^{-/-} phenotype was independent of genetic background

K.-H. Herzog and J. I. Morgan, Department of Developmental Neurobiology, St. Jude Children's Research Hospital, 332 North Lauderdale, Memphis, TN 38101, USA. M. J. Chong, M. Kapsetaki, P. J. McKinnon, Department of Genetics, St. Jude Children's Research Hospital, 332 North Lauderdale, Memphis, TN 38101, USA.

*To whom correspondence should be addressed. E-mail: peter.mckinnon@stjude.org

Fig. 1. Absence of ionizing radiation-induced apoptosis in regions of the *Atm*^{-/-} CNS. Neutral red-stained sections of P3 *Atm*^{-/-} cerebellum (C) and P5 retina (E) show a pronounced lack of pyknotic nuclei compared with similar sections from irradiated WT tissues (B and D). (A) Unirradiated WT cerebellum. (F to L) ISEL staining in the EGL of unirradiated WT (F), irradiated *Atm*^{-/-} (G), and irradiated WT mouse (H and I) at P3. ISEL staining in (I) coincides with cells in the EGL having the morphological characteristics of apoptosis. In contrast, apoptosis is absent from unirradiated thymus (J), but present in irradiated WT (K) and *Atm*^{-/-} (L) mice. Magnification: ×85 (A to H); ×170 (I to L). Differences in apoptosis in the P3 CNS of *Atm*^{-/-} and WT mice after irradiation were also found for the dentate gyrus and regions of the cerebral cortex.



(12), we performed the irradiation experiment with mice from each contributing genotype, 129/svj and C57BL/6. Similar spatial and temporal patterns and levels of death were observed after irradiation in each strain. We also studied cell death in the

dentate gyrus of irradiated *Atm*^{-/-} mice up to 48 hours after irradiation and still did not detect cell death, indicating that apoptosis was not simply delayed in the *Atm*^{-/-} mice (Fig. 2). Taken together, our data support the conclusion that *Atm* mediates ionizing radiation-induced apoptosis in the developing CNS.

The p53 gene product is required for ionizing radiation-induced apoptosis in thymocytes and cerebellar granule neurons (13, 14), and p53 induction in irradiated cell lines derived from AT individuals and *Atm*^{-/-} mice is delayed or absent (15). Therefore, we examined whether p53 is involved in *Atm*-dependent apoptosis. We found reduced p53 induction in the CNS of *Atm*^{-/-} mice after irradiation as measured by protein immunoblot analysis and immunohistochemistry (16). Protein immunoblot analysis showed a lack of p53 stabilization in the cerebral cortex, olfactory bulb, and hippocampus and only a weak induction in the cerebellum from *Atm*^{-/-} mice compared with marked up-regulation in WT mice (Fig. 3A). However, induction of p53 was apparent in the thymus of both WT and *Atm*^{-/-} mice, consistent with p53-dependent, but *Atm*-independent, death after γ -irradiation in this organ. Additionally, immunohistochemistry showed p53 induction after irradiation localized to regions of the cerebellum that subsequently undergo apoptosis (Fig. 3B). *p53*^{-/-} mice (17) were also resistant to irradiation-induced cell death in the developing nervous system, supporting the notion that *Atm*-dependent death in the CNS requires p53 (Fig. 3Cb). Because ATM interacts with c-Abl (18) and c-Abl can regulate apoptosis after ionizing radiation (19), c-Abl null mice (20) were also examined. Cell death in the CNS of c-Abl null mice was indistinguishable from that in WT mice after irradiation (Fig. 3C). Thus, *Atm* is an upstream modulator of apoptosis in the CNS after γ -irradiation and most likely signals by way of p53, but independently of c-Abl.

Although no widespread cell death was observed in the developing postnatal *Atm*^{-/-} CNS after γ -irradiation, two populations of neural cells still underwent apoptosis in the *Atm*^{-/-} mice. In the irradiated WT eye, apoptotic cells were seen throughout the periphery and center of the retina, whereas apoptosis was seen only in the periphery of irradiated *Atm*^{-/-} retina. Cell death was also apparent in the subventricular zone (SVZ) of both WT and *Atm*^{-/-} mice, although it was reduced in the *Atm*^{-/-} mice. Both the SVZ and the marginal zone of the retina contain relatively undifferentiated, multipotent precursors capable of giving rise to both neurons and glia (21). In contrast, the

Fig. 2. Absence of cell death in the dentate gyrus of *Atm*^{-/-} mice up to 48 hours after irradiation. After ionizing irradiation, the developing P5 dentate gyrus of WT mice (+/+) show typical pyknosis after 24 hours (A) and extensive cell depletion after 48 hours (B). However, P5 *Atm*^{-/-} dentate gyrus demonstrates marked resistance to irradiation for up to 48 hours (C and D), with no detectable pyknosis or obvious cell loss.

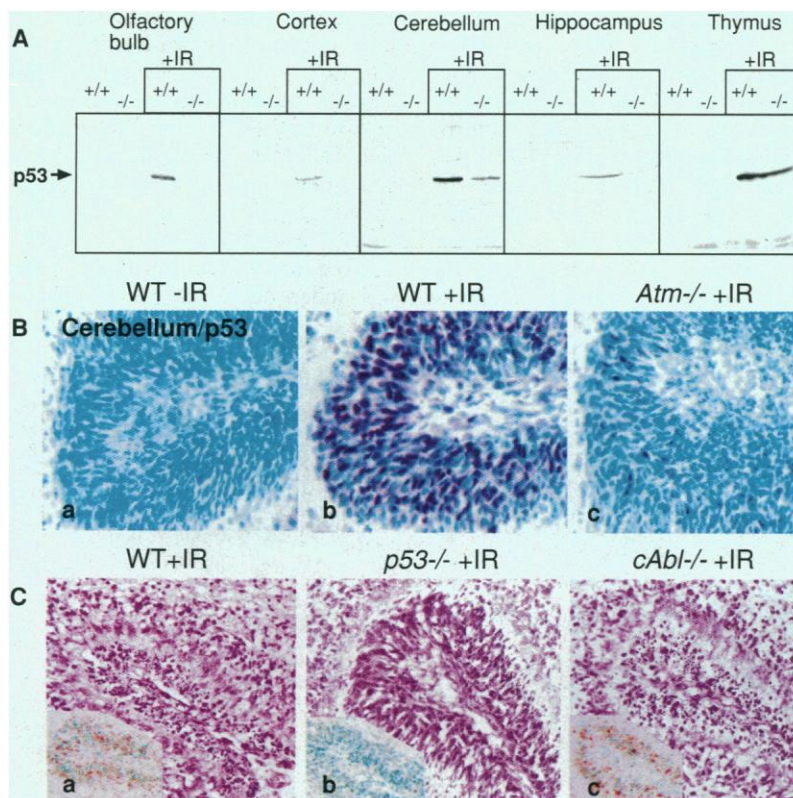
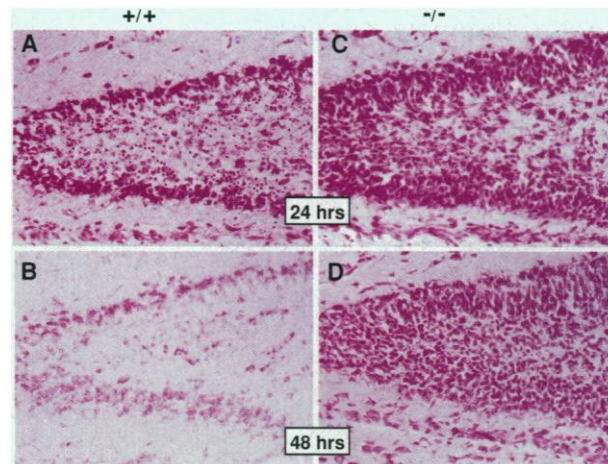


Fig. 3. *Atm*-dependent apoptosis coincides with p53 stabilization. (A) Protein immunoblot analysis of p53 after ionizing radiation in the P5 CNS of WT and *Atm*^{-/-} mice. In all WT (+/+) CNS tissues, p53 stabilization is apparent 2 hours after ionizing radiation, whereas *Atm*^{-/-} tissues (-/-) show a pronounced deficit in p53 stabilization, although p53 stabilization in the thymus is similar in WT and *Atm*^{-/-} mice. +IR: Tissue from irradiated animals. (B) Immunohistochemical localization identifies p53 stabilization in granule cells of the cerebellar EGL in WT, but not *Atm*^{-/-} mice after irradiation. p53 stabilization in the cerebellar EGL coincides with cells in these regions that subsequently undergo apoptosis (Fig. 1). (a) Unirradiated (-IR) WT, (b) irradiated (+IR) WT, and (c) irradiated *Atm*^{-/-} cerebellum. (C) Neutral red-stained cerebellum from irradiated WT (a), p53 null (b), and c-Abl null mice (c) show that WT and c-Abl mice undergo irradiation-induced apoptosis, whereas p53 null mice do not. (Insets) ISEL-stained cerebellum of the respective genotypes. A similar lack of apoptosis was found in the retina and dentate gyrus after irradiation in *p53*^{-/-} mice, but not *c-Abl*^{-/-} or WT mice.

cerebellar EGL and the dentate gyrus harbor neuroblasts that generally give rise to a single lineage (22). Thus, as cells move from a multipotent, less-differentiated state to their terminal phenotype, *Atm* function after irradiation becomes apparent. Because *Atm*^{-/-} and *p53*^{-/-} mice appear neuroanatomically normal (23), *Atm*- and *p53*-dependent apoptosis is probably distinct from programmed cell death occurring during nervous system development (24).

These data establish a role for *Atm* during radiation-induced apoptosis in select cell populations in the developing CNS. It is possible, at this stage, that neurons require *Atm* as a component of a survival checkpoint so that developing neural cells that have genomic (or other) damage can be eliminated. Thus, defective *Atm* may allow genomically compromised neurons to survive, and their accumulated mutations lead to functional deficits later in life. In specific cell populations such as Purkinje or granule cells, this process could lead to selective neurodegeneration as seen in AT (3). Further, because disruption of *Atm* function is protective against irradiation, these findings may have therapeutic implications for attenuating the serious neurological sequelae after craniospinal irradiation for pediatric brain tumors.

REFERENCES AND NOTES

1. K. Savitsky et al., *Science* **268**, 1749 (1995).
2. M. F. Lavin, Y. Shiloh, *Annu. Rev. Immunol.* **15**, 177 (1997).
3. R. P. Sedgwick and E. Boder, in *Handbook of Clinical Neurology*, P. Vinken, G. Bruyn, H. Klawans, Eds. (Elsevier, New York, 1991), vol. 60, pp. 347–423.
4. P. J. McKinnon, *Hum. Genet.* **75**, 197 (1987).
5. G. Rotman and Y. Shiloh, *Bioessays* **19**, 911 (1997).
6. N. Heintz, *Curr. Opin. Neurol.* **9**, 137 (1996).
7. H. A. Soares, J. I. Morgan, P. J. McKinnon, *Neuroscience*, in press; G. Chen and E. Lee, *J. Biol. Chem.* **271**, 33693 (1996).
8. The *neo* gene was used to interrupt exon 57 and replace exon 58 of *Atm* (Genbank number U55702), deleting a region of the phosphoinositol 3-kinase domain as occurs in a number of individuals with AT.
9. C. Barlow et al., *Cell* **86**, 159 (1996); A. Elson et al., *Proc. Natl. Acad. Sci. U.S.A.* **93**, 13084 (1996); Y. Xu and D. Baltimore, *Genes Dev.* **10**, 2401 (1996). However, we (M.J.C. and P.J.McK.) do not find abnormalities in the *Atm*^{-/-} cerebellum using electron microscopy as has been reported by R. O. Kuljis, Y. Xu, M. C. Aguilu, and D. Baltimore [*Proc. Natl. Acad. Sci. U.S.A.* **94**, 12688 (1997)].
10. Wild-type (*Atm*^{+/+}) or *Atm*^{-/-} littermates were used at either 3 or 5 days after birth (P3 or P5; day of birth is P0). Mice were irradiated with 14 gray (Gy) from a Cs irradiator (delivered at a rate of 0.9 Gy/min) and allowed 18, 24, or 48 hours of recovery. Tissues were collected after fixation by transcardial perfusion with 4% paraformaldehyde and subsequently cryoprotected in sucrose and cryosectioned (12-μm coronal sections). Neutral red staining was performed with 1% Neutral red (Aldrich Chemical) in 0.1 M acetic acid (pH 4.8) for 1 min followed by dehydration in ethanol. All data presented compare littermates and are derived from 10 separate litters. All animal experiments were performed according to institutional guidelines and under an Institutional An-

imal Care and Use Committee (IACUC)-approved protocol.

11. Y. Gavrieli, Y. Sherman, S. A. Ben-Sasson, *J. Cell Biol.* **119**, 493 (1992). ISEL staining was performed on tissue cryosections from P3 animals, 18 hours after irradiation with the FragEL kit (Oncogene Research Products) according to the manufacturer's directions. Sections were counterstained with methyl green (Vector Laboratories).
12. P. E. Schauwecker and O. Steward, *Proc. Natl. Acad. Sci. U.S.A.* **94**, 4103 (1997).
13. S. W. Lowe, E. M. Schmitt, S. W. Smith, B. A. Osborne, T. Jacks, *Nature* **362**, 847 (1993); A. R. Clarke et al., *ibid.*, p. 849.
14. K. A. Wood and R. J. Youle, *J. Neurosci.* **15**, 5851 (1995); Y. Enokido, T. Araki, K. Tanaka, S. Aizawa, H. Hatanaka, *Eur. J. Neurosci.* **8**, 1812 (1996).
15. M. B. Kastan et al., *Cell* **71**, 587 (1992). A delay or absence of *p53* stabilization has been reported in irradiated thymocytes from *Atm*^{-/-} mice resulting in reduced or normal levels of apoptosis, respectively [C. H. Westphal et al., *Nature Genet.* **16**, 397 (1997); C. Barlow, K. D. Brown, C. X. Deng, D. A. Tagle, A. Wynshaw-Boris, *ibid.* **17**, 453 (1997)].
16. Tissues were harvested 2 hours after 14 Gy of irradiation and homogenized in SDS sample buffer; equal quantities of protein were separated on 10% SDS-polyacrylamide gel electrophoresis gels and transferred to nitrocellulose membranes. Membranes were stained with Ponceau S (Sigma) to confirm equal protein transfer. *p53* was detected with antibody to *p53* (anti-*p53*) (Ab-7, Calbiochem) at a dilution of 1/2500 for 1 hour at room temperature. Antibody binding was detected by enhanced chemiluminescence (Amersham). *p53* immunohistochemistry was done with anti-*p53* (CM5, Vector Laboratories) at a dilution of 1/500 by antigen retrieval [C. A. Midgley et al., *J. Cell Sci.* **101**, 183 (1992)]. The Vectastain Elite ABC kit-VIP substrate avidin-biotin

immunoperoxidase system (Vector Laboratories) was used for visualization of primary antibody binding. Sections were counterstained with methyl green. Data were from five separate litters.

17. *p53*^{-/-} mice were obtained from Jackson Laboratories (Bar Harbor, Maine) and are described in (13). Experiments were performed twice with littermates (*p53*^{+/+} and *p53*^{-/-}) from two separate litters.
18. R. Baskaran et al., *Nature* **387**, 516 (1997); T. Shafman et al., *ibid.*, p. 520.
19. Z. M. Yuan et al., *Proc. Natl. Acad. Sci. U.S.A.* **94**, 1437 (1997).
20. V. L. Tybulewicz, C. E. Crawford, P. K. Jackson, R. T. Bronson, R. C. Mulligan, *Cell* **65**, 1153 (1991).
21. D. A. Steindler, T. Kadrie, H. Fillmore, L. B. Thomas, *Prog. Brain Res.* **108**, 349 (1996); C. Lois, A. Alvarez-Buylla, *Proc. Natl. Acad. Sci. U.S.A.* **90**, 2074 (1993); D. L. Turner and C. L. Cepko, *Nature* **328**, 131 (1987).
22. M. E. Hatten and N. Heintz, *Annu. Rev. Neurosci.* **18**, 385 (1995); W. M. Cowan, B. B. Stanfield, K. Kishi, *Curr. Top. Dev. Biol.* **15**, 103 (1980).
23. Although *p53*^{-/-} mice are viable, a significant subset of *p53*^{-/-} embryos develop defects in neural tube closure [J. F. Armstrong, M. H. Kaufman, D. J. Harrison, A. R. Clarke, *Curr. Biol.* **5**, 931 (1995); V. P. Sah et al., *Nature Genet.* **10**, 175 (1995)].
24. R. W. Oppenheim, *Annu. Rev. Neurosci.* **14**, 453 (1991).
25. We thank S. Goff and S. Boast (Columbia University) for providing *c-Abl* null mice, C. Nagy for help in generating the *Atm*^{-/-} mice, and S. J. Baker for comments on the manuscript. Supported by the AT Children's Project (P.J.McK.), Cancer Center CORE grant CA-21765, and by the American Lebanese and Syrian Associated Charities (ALSAC) of St. Jude Children's Research Hospital.

27 January 1998; accepted 27 March 1998

COI1: An Arabidopsis Gene Required for Jasmonate-Regulated Defense and Fertility

Dao-Xin Xie, Bart F. Feys,* Sarah James,†
Manuela Nieto-Rostro, John G. Turner‡

The *coi1* mutation defines an *Arabidopsis* gene required for response to jasmonates, which regulate defense against insects and pathogens, wound healing, and pollen fertility. The wild-type allele, *COI1*, was mapped to a 90-kilobase genomic fragment and located by complementation of *coi1-1* mutants. The predicted amino acid sequence of the *COI1* protein contains 16 leucine-rich repeats and an F-box motif. It has similarity to the F-box proteins *Arabidopsis* TIR1, human Skp2, and yeast Grr1, which appear to function by targeting repressor proteins for removal by ubiquitination.

Jasmonates (JAs), which include jasmonic acid and its cyclopentanone derivatives, are widely distributed throughout the plant kingdom. They are synthesized by the octadecanoic pathway from linolenic acid in undamaged tissues and (apparently) by a different pathway in wounded tissues. JAs affect a variety of processes in plants, including root growth, fruit ripening, senes-

cence, pollen development, tuber formation, tendril coiling, and defense against insect pests and pathogens. They alter gene transcription, RNA processing, and translation (1).

Tomato plants respond to injury, such as that caused by chewing insects, by making proteinase inhibitor (pin) proteins that inhibit insect digestive proteases (2). JA is required for plant defenses against insect predation (3) and acts together with ethylene formed in the wounded tissues to regulate pin gene expression (4). In *Arabidopsis*, the functions of JA are defined by the triple mutant *fad3-2 fad7-2 fad8*, which is deficient in linolenic acid,

School of Biological Sciences, University of East Anglia, Norwich NR4 7TJ, UK.

*Present address: Sainsbury Laboratory, John Innes Centre, Norwich, UK.

†Present address: Biological Sciences, Wye College, Wye, Ashford, Kent, UK.

‡To whom correspondence should be addressed.